

Effect of processing conditions on water mobility and cooking quality of gluten-free
pasta. A Magnetic Resonance Imaging study

Alessandra Marti*, Enzo Maria Ragg, Maria Ambrogina Pagani

Department of Food, Environmental, and Nutritional Sciences (DeFENS)

Università degli Studi di Milano - Via Celoria, 2, 20133 Milan, Italy

*Corresponding author:

alessandra.marti@unimi.it

1 **Abstract**

2 A new approach for producing gluten-free pasta from hydrated (50 °C, 20 min) rice
3 kernels, skipping the grinding step, was explored. Magnetic Resonance Imaging
4 (MRI) was used to study the hydration kinetics of rice, by monitoring the time
5 evolution of both proton density and water transverse-relaxation rate during water
6 diffusion. Results showed that the optimal water diffusion was reached after 180 min,
7 allowing the extrusion of hydrated rice kernels into pasta. MRI analysis also
8 highlighted in cooked pasta gradients of water distribution and mobility, in agreement
9 with the high shear force that was measured using the Kramer cell (1066.5 vs 896.4
10 N). The high hydration in the external layers of pasta did not negatively affect the
11 cooking quality (cooking loss, compression energy, firmness) of the product. MRI
12 analysis provided an experimental evidence for the optimization of early steps in the
13 technological process of grains for the production of gluten-free pasta.

14

15

16 **Keywords:** Magnetic resonance imaging; gluten-free pasta; rice kernel hydration;
17 parboiling; cooking quality

18 **1. Introduction**

19 Gluten-free (GF) dried pasta can be mainly prepared using two approaches (Marti &
20 Pagani 2013). The first one focuses on the use of pregelatinised GF raw materials
21 (starches and/or flours), in which starch is already mostly gelatinized. Here, the pre-
22 treated raw materials can be formed into pasta by the same extrusion press and
23 conditions commonly used in durum wheat pasta plant. This way is surely
24 characterised by low investment costs related to the technology but relatively high
25 costs for the raw materials (Marti & Pagani 2013). In the second approach – namely
26 cooking-extrusion process - native flour is treated with steam and extruded at high
27 temperatures (more than 100 °C) for promoting a relevant gelatinization of starch
28 granules directly inside the cooker-extruder. Cooking-extrusion of native rice did not
29 seem to be efficacious in creating a continuous and smoothed starchy matrix, which
30 instead resulted in the disruption of the surface structure during cooking and thus in
31 low firmness (Marti, Caramanico, Bottega & Pagani, 2013). On the contrary, the
32 extrusion of a pre-treated flour (i.e. parboiled rice) in the cooking-extruder induced a
33 new starch organization, assuring a good texture in the cooked product and avoiding
34 additives (Marti, Seetharaman & Pagani, 2010). In addition to the technological
35 aspects, parboiled rice resulted in improved nutritional properties compared to milled
36 rice. Indeed, during the process part of vitamins and minerals migrate towards the
37 endosperm (Bhattacharya, 2004), and resistant starch is formed (Casiraghi, Brighenti,
38 Pellegrini, Leopardi & Testolin, 1993).

39 The role of formulation and processing conditions on structural and cooking
40 quality (Mariotti, Iametti, Cappa, Rasmussen & Lucisano, 2011; Lucisano, Cappa,
41 Fongaro & Mariotti, 2012; Marti, Barbiroli, Marengo, Fongaro, Iametti & Pagani,
42 2014) and nutritional properties (Marti, Abbasi Parizad, Marengo, Erba, Pagani &

43 Casiraghi, 2017) have been recently addressed. In particular, differences in starch
44 digestibility might be driven by differences in biopolymer interactions promoted
45 during processing. At this regard, the effects of pasta-making processing on starch-
46 starch (Marti et al., 2010; Marti, Pagani & Seetharaman, 2011a; Marti, Pagani &
47 Seetharaman, 2011b) and starch-protein (Barbiroli, Bonomi, Casiraghi, Iametti,
48 Pagani & Marti, 2013; Cabrera-Chavez et al., 2012) interactions in GF pasta has been
49 investigated in previous studies. On the other hand, to the best of our knowledge no
50 information on starch-water interaction is available in a non-gluten system. Thus, this
51 study aims at assessing water mobility in GF pasta using Magnetic Resonance
52 Imaging (MRI), that has successfully been used in the past for semolina pasta
53 (Horigane, Kawabuchi, Uchijima & Yoshida, 2009; Bonomi et al., 2012).

54 In addition, in the view of process simplification, this study proposes a new
55 approach for producing GF pasta directly from parboiled rice kernels, after their
56 hydration, skipping the grinding step. In fact, although the grinding of rice is a simple
57 and easy step, it is inevitably associated with the formation of dust that can favor the
58 infestation of pests and increase the risk of explosions (Posner & Hibbs, 2005). MRI
59 was used to assess kernel hydration properties useful to choose the processing
60 conditions of pasta production. Finally, the effect of processing conditions on cooking
61 behavior, starch properties and water mobility of cooked pasta was also investigated.

62 **2. Materials and Methods**

63 **2.1 Raw materials**

64 Indica rice (*Oryza sativa* L.; starch: 85%; amylose: 25 g/100 g total starch) of
65 commercial origin was used in this study. Parboiled milled rice kernels - henceforth
66 RK – and the related flour - henceforth RF - were kindly provided by Riso Viazzo
67 s.r.l., (Crova, Italy). Starch (80.9 g in 100 g dry matter), protein (10.7 g in 100 g dry

68 matter), lipids (0.4 g in 100 g dry matter), and ash (0.9 g in 100 g dry matter) content
69 of RK were determined using the standard AACC methods (AACCI, 2001).

70 **2.2 Pasta samples**

71 Pasta (20 kg) from RF - henceforth PaRF - was prepared as reported by Marti et al.
72 (2010), with little modification (Fig. S1). The mixture of flour and water (with a final
73 water content of 40%) was extruded in a Progel[®] extruder (single screw; Braibanti,
74 Milano, Italy) fed with steam at 150 kg/h and 130 °C. After the first extrusion step,
75 the pellets from heat-treated dough were formed in a macaroni shape in the
76 continuous extruder (45 °C) used for the conventional process (Braibanti, Milano,
77 Italy).

78 RK were soaked in tap water for 20 min at 50 °C (kernel:water ratio = 1:1.5). After
79 removing the excess of water, the kernels were tempered for 3 hours at 22 °C keeping
80 the kernels in sealed containers to avoid moisture changes. Rice kernels were then
81 formed into pasta - henceforth PaRK - as described above. Both pasta samples (PaRF
82 and PaRK) were dried in an experimental drying cell (Braibanti, Milan, Italy) using a
83 low-temperature drying cycle (50 °C for 14 hours) and stored at room temperature
84 until analyzed. Before the analysis, rice pasta samples were ground obtaining a
85 product with less than 500 µm particle size.

86 **2.3 Magnetic Resonance Imaging (MRI)**

87 MRI experiments were carried out on both rice kernels after their hydration and
88 cooked pasta.

89 Five grams of rice grains were soaked at 50 °C in distilled water (kernel:water ratio =
90 1:1.5). After 20 min of soaking, grains were removed, drained for 1 min and blotted
91 with filter paper to remove any excess water attached to the surface. The blotted

92 grains were inserted into NMR tubes (diameter: 10 mm) for MRI experiments that
93 were performed up to 265 min of tempering time.

94 MRI studies of rice kernels and cooked pasta were carried out using a standard bore
95 Bruker Avance AV600 spectrometer (Bruker Biospin GmbH, Rheinstetten, Germany)
96 equipped with a 10 mm ^1H micro-imaging probe and a variable temperature control
97 unit. The magnetic field strength was 14 T, corresponding to a ^1H resonance
98 frequency of 600.1 MHz. A series of MRI slices of rice/pasta samples was taken at
99 room temperature with the following acquisition parameters: MSME (Multi Slice
100 Multi Echo) acquisition; number of slices from image: 8; thickness: 0.3 mm; no slice
101 separation; repetition time: 800 ms; echo time 3.2 ms; number of echoes: 8; number
102 of scans: 8; total acquisition time: 15min. Field of view was set to $9\times 9\text{ mm}^2$, with a
103 matrix size 128×128 units, corresponding to an in-plane resolution of $70\times 70\text{ }\mu\text{m}^2$. For
104 each slice, T_2 values were extracted by a multi-parametric non-linear fitting
105 ($y=A+B\cdot e^{-t/T_2}$) of the intensity decays and used for reconstruction of the
106 corresponding parametric images. Acquisition, data processing and image analysis
107 were performed with ParaVision v.4.0 (Bruker BioSpin MRI GmbH, Ettlingen,
108 Germany). Non-linear least squares fitting analysis of MRI data was performed with
109 OriginPron 2016 (OriginLab Corporation, Northampton, MA, USA).

110 **2.4 Pasta quality indices**

111 A colorimeter (CR 210, Minolta Co., Osaka, Japan) was used to measure the lightness
112 (L^*) and saturation of the color intensity value (a^* , redness-greenness; b^* ,
113 yellowness-blueness) of flours, using the CIE $L^*a^*b^*$ color scale. The measurement
114 was replicated five times and the average value was used.

115 Cooking behavior was evaluated by determining the grams of solid lost into
116 cooking water for 100 g of dry pasta, at a pasta:water ratio = 1:10 with no salt

117 addition. After cooking, pasta was drained, water was brought back to the initial
118 volume, and an aliquot was dried to constant weight at 105°C. Weight increase of
119 pasta due to water absorption during cooking was evaluated gravimetrically.

120 Texture measurements were carried out using a Texture Z005 (Zwick Roell, Ulm,
121 Germany), equipped with a Kramer Shear Cell. An aliquot of pasta (25 g) was cooked
122 in 250 ml distilled water till the optimal cooking time (OCT). After cooking, pasta
123 was drained for 60 s, cooled under water for 30 s and drained one more time for 60 s.
124 Pasta samples were analyzed after 10 min of rest at room temperature in a sealed
125 container. Firmness (N, expressed as the maximum force necessary to pack the
126 sample), compression energy (N*mm, corresponding to the area of the curve until the
127 maximum force), and shear force (N, expressed as the force necessary so that blades
128 pass through the sample) were automatically calculated by the software provided with
129 the instrument. Average data of 10 replicates for each sample were reported.

130 **2.5 Micro-Visco-AmyloGraph (MVAG)**

131 Pasting properties were measured in duplicate in a Micro-Visco-AmyloGraph device
132 (Brabender, Duisburg, Germany), on samples ground to particles smaller than 0.5
133 mm. An aliquot of 15 g of the sample was dispersed in 100 mL of distilled water,
134 scaling both flour and water weight on a 14% flour moisture basis. The pasting
135 properties were evaluated under constant conditions (speed: 250 rpm by using the
136 following temperature profile: heating from 50 °C up to 95 °C; holding at 95 °C for
137 30 min; cooling from 95 °C to 50 °C; holding at 50 °C for 30 min, and cooling from
138 50 °C to 30 °C). The heating and cooling phases were carried out with a temperature
139 gradient of 3 C/min. Data were elaborated as reported by Mariotti et al. (2011).

140 **2.6 Statistical analysis**

141 T-test was used for comparing the average of pasta samples for color and cooking
142 behavior. Analysis of variance (ANOVA) was performed for MVAG indices, utilizing
143 Statgraphics XV version 15.1.02 (StatPoint Inc., Warrenton, VA, USA). Samples
144 were used as a factor. When the factor effect was found to be significant ($p \leq 0.05$),
145 significant differences among the respective means were determined using Fisher's
146 Least Significant Difference (LSD) test.

147 **3. Results and Discussion**

148 **3.1 Water distribution in rice kernels before and after hydration by MRI**

149 MRI was used to determine the optimal tempering time to allow homogeneous water
150 distribution in RK before pasta processing. Indeed, this technique directly detects the
151 protons of the water molecules and generates images with good spatial resolution. The
152 relative intensities of the pixels can be rendered quantitatively reliable as long as
153 appropriate protocols are used to acquire and process the data (Takeuchi, Maeda,
154 Gomi, Fukuoka, & Watanabe, 1997).

155 To date, several MRI investigations have been applied to rice and other grains to
156 monitor various changes in the physical structure and moisture distribution during or
157 after cooking (Gruwel, Chatson, Yin & Abrams, 2001; Hong et al., 2009). Moreover,
158 MRI technique has successfully been used to discriminate between free and bound
159 water, and to assess meanwhile the total amount of water present in foods, including
160 pasta (Takeuchi et al., 1997; Horigane et al., 2009; Bonomi et al. 2012).

161 Fig. 1 shows the water distribution in parboiled rice, measured in 0.3 mm slices from
162 the image, as function of the resting time of soaked kernels in water for 20 min. In
163 these images, each MRI pixel intensity is proportional to the water content of the
164 corresponding rice voxel. The graduation in the grayscale intensities seen within the
165 rice grains reveals that water is not evenly distributed. Initially, it is mainly present in

166 an outer layer of the rice kernel. Then, water slowly diffuses into the core, reaching an
167 equilibrium state after at least 3 hours, where it appeared to be homogeneously
168 distributed and the distinction between outer and inner layers is no more apparent.
169 As the MRI images were taken from a “multi-slice-multi-echo” experiment, it was
170 possible to derive the distribution of the water transverse relaxation rate (T_2) within
171 each slice, as depicted by the parametric image of Fig. 2. As it has been shown
172 elsewhere (Takeuchi et al., 1997), T_2 values are directly related to water mobility at a
173 molecular level (Carini, Curti, Littardi, Luzzini, & Vittadini, 2013). In our rice
174 samples, values span in the interval between 10ms (blue pixels) and 50ms (red
175 pixels). Such values are typical for water molecules hydrogen-bonded to
176 macromolecular matrix, whereas values greater than 100 ms are in general more
177 related to freely diffusible water.

178 A comparison between the two MRI images in Fig. 1 and 2 proves that there is an
179 initial external layer of tightly bound water, arising from the macromolecular
180 network, mainly composed by amylose and amylopectin, hydrated during the
181 parboiling process (blue regions). Such regions do not change their state during the
182 diffusion process. By contrast, inner regions initially define a not-yet-hydrated core
183 with a low proton density. At the interface with the external layer, some residual
184 water is evident with a mobility even higher than the external layer (pixels in green to
185 red color, $T_2 > 30$ ms), corresponding to mobile water not entrapped within the starch
186 crystallites. As water diffuses from the outer regions into the rice kernel core, the low-
187 hydration regions reduce in size and are gradually replaced by such higher mobility
188 water regions.

189 MRI images thus provide an experimental basis for a quantitative determination of the
190 kinetics of hydration pathways. The MRI proton density images were quantified by

191 measuring the integrated pixel intensity of the inner region in two rice kernels, chosen
192 according to their orientation within a single slice (long or short axis; see Fig. 1),
193 while the T_2 parametric images were analyzed by pixel count of the blue channel in
194 the RGB image ($T_2 < 10$ ms).

195 As shown in Fig. 3A, hydration, measured from the MRI proton density images,
196 might be modelled by a 1st order kinetics, according to the following mono-
197 exponential equation:

$$I = I_0 + I_1(1 - e^{-kt})$$

198 Where I is the integrated intensity of the MRI area under examination, I_0 and I_1 are
199 the initial and final integrated intensities, respectively, and k is the 1st order kinetics
200 time constant of water diffusion. The parameters derived by a non-linear least-squares
201 fit analysis depend on the section of the rice kernel taken into consideration:

202 (direction 1, long axis) $I_0 = 13.1 \pm 0.8\%$; $I_1 = 24.6 \pm 0.8\%$; $k = 0.010 \pm 0.001 \text{ min}^{-1}$;

203 (direction 2, short axis) $I_0 = 3.2 \pm 0.5\%$; $I_1 = 9.3 \pm 0.5\%$; $k = 0.015 \pm 0.002$. The time

204 constants are the most interesting parameters, as they can directly be related to the

205 water diffusion process. On the other hand, water mobility (see Fig. 3B) follows a

206 different time course, as it proceeds with a sigmoidal-shape plot, reminiscent of a

207 cooperative behavior. The time course might be modelled according to the following

208 equation:

$$A = A_0 + (A_1 - A_0)/(1 + 10^{(c-t)^p})$$

209

210 The following parameters were thus derived: A_0 (bottom asymptote) = $63.6 \pm 0.9\%$; A_1

211 (top asymptote) = $96.2 \pm 0.9\%$; c (center) = 157.7 ± 2.2 min; p (Hill slope) = $0.073 \pm$

212 0.02 . Actually, an abrupt change in water mobility occurs between 148 min and 170

213 min. At 180 min water mobility can be considered completely stabilized in a tightly

214 bound status up to a 96% level. For this reason, the optimal resting time for rice
215 kernel soaking was considered to be at least 180 min.

216 **3.2 Pasta Quality**

217 Pictures of pasta samples are reported in Fig. S1. From a qualitative standpoint, both
218 samples appeared omogeneous and appealing in terms of color and structure. From a
219 quantitative standpoint, pasta-making process did not affect the products luminosity
220 (Table 1), whose values were similar to pasta from durum wheat semolina (Marti et
221 al., 2013). PaRF and PaRK significantly differed for both a^* and b^* values, with
222 PaRK exhibiting higher redness and lower yellowness than PaRF. Differences in color
223 might be due to the soaking step. Loss of pigment into the soaking water should be
224 taken into consideration, as shown in the study of Lamberts, Brijs, Mohamed,
225 Verhelst & Delcour (2006). Both pasta samples presented lower luminosity and
226 higher yellowness than commercial 100% rice pasta (Marti et al., 2013). This result is
227 due to the use of parboiled rice as raw material. As well-known, the darker and more
228 yellow color after parboiling is a consequence of the migration of pigments from the
229 husk and/or bran to the endosperm (Bhattacharya & Ali, 1985) and non-enzymatic
230 browning (Dendy, 2000). The impact of different hydration kinetics in flour vs
231 kernels might also play a role in color differences.

232 No differences in cooking time were detected between the samples (Table 1). This is
233 valid also for leaching into cooking water and water absorption, which values were
234 not significantly different between PaRF and PaRK (Table 1). Because of the lack of
235 a gluten network in all gluten free pasta, starch polymers were less efficaciously
236 entrapped in the matrix in comparison with semolina pasta, resulting in a product with
237 a high cooking loss, even three-four times more than that of the semolina sample
238 (Marti et al., 2013). A decrease in starch leaching during cooking can be promoted by

239 the adding texturing proteins (Marti et al., 2014) or emulsifiers (Lai, 2002).
240 As regards textural properties, no significant differences ($p < 0.05$) were measured in
241 terms of firmness and compression energy. On the other hand, PaRK exhibited a
242 significant ($p < 0.05$) higher shear force than PaRF. Processing conditions (e.g.
243 extrusion temperature) adopted during the extrusion-cooking step should be optimized
244 in order to decrease the extreme firmness of the product. Indeed, experimental pasta
245 samples exhibited firmness values even two-fold higher than those of commercial
246 semolina pasta (data not shown).

247 **3.3 Pasting Properties**

248 The MVAG test is widely used for evaluating the changes in viscosity of cereal flours
249 or starches during heating and cooling. This approach has also been successfully used
250 on conventional pasta to assess the contribution of macromolecules interactions and
251 of temperature-dependent structural changes on finely ground pasta (Bonomi et al.,
252 2012; Marti et al., 2014). It has been also used on non-conventional pasta, providing
253 information on molecular changes promoted by pasta-making process (Marti et al.,
254 2010; Marti et al., 2013) and/or ingredients (Marti, Pagani & Seetharaman, 2011c;
255 Cabrera-Chavez et al., 2012). The pasting properties of rice flour and pasta samples
256 are shown in Fig. S2 and the related indices in Table 1. Pasting temperature was lower
257 in PaRK than PaRF, likely indicating that the extrusion step was more effective in
258 starch gelatinization in hydrated rice kernels compared to flour, probably due to the
259 high water availability in soaked kernels. Indeed, the higher the degree of
260 gelatinization, the lower the pasting temperature (Marti et al., 2013). Moreover, PaRK
261 showed a higher maximum viscosity than PaRF (Table 1) suggesting greater starch
262 swelling ability, likely related to faster hydration and water absorption during cooking
263 (data not shown). Finally, during cooling at 30°C, PaRK exhibited higher setback

264 values suggesting greater retrogradation tendency, likely explaining the high shear
265 force of the cooked product (Table 1). Our results confirmed previous studies that
266 stated that the setback value was positively related with the firmness of rice noodles
267 (Bhattacharya, Zee & Corke, 1999) and rice pasta (Marti et al., 2010).

268 **3.2 Water distribution in rice pasta by MRI**

269 The same kind of MRI measurements used for monitoring grain hydration kinetics
270 during soaking were then performed on the two kinds of experimental rice pasta PaRF
271 and PaRK, in order to ascertain whether differences in the processing of rice kernels
272 might affect the quality of the obtained pasta.

273 Fig. 4 shows both the water distribution and mobility in the two pasta samples after
274 cooking at optimal time (15 min). Pasta samples exhibited some differences,
275 especially at the surface layer, where the PaRK sample seems to be more hydrated
276 than PaRF. Differences in water mobility were confirmed by measuring the spin–spin
277 relaxation time (Fig. 5). Both pasta types present a non-uniform dispersion of T_2 -
278 values, indicating the presence of at least three distinct regions with different water
279 mobilities: (a) low water mobility ($T_2 = ca. 15$ ms); (b) intermediate water mobility
280 ($T_2 = 25$ ms); (c) high-mobility water ($T_2 = 30$ ms). In particular, group (a) is equally
281 present in both PaRF and PaRK samples, whereas in the PaRK sample there is an
282 evident shift in population from group “b” to group “c” (high-mobility), consistent
283 with the increase in hydration observed in the external layer of this kind of pasta.
284 Gradients of water distribution and mobility in conventional pasta from durum wheat
285 semolina have been positively related to the “al dente” feeling in cooked pasta
286 (Horigane et al., 2009; Bonomi et al., 2012). This result is in agreement with the
287 higher shear force measured in PaRK compared to PaRF (Table 1).

288 **4. Conclusions**

289 In this paper we have shown that MRI is able to provide an experimental basis for the
290 quantitative analysis of the kinetics of hydration pathways, by monitoring the time
291 evolution of both proton density and water transverse-relaxation rate during moisture
292 diffusion in non-spherically shaped samples, such as the parboiled rice kernels. The
293 MRI analysis thus provided an experimental evidence for the optimization of
294 important early steps in the technological process of parboiled rice for the production
295 of rice flour-based pasta.

296 Results on the overall pasta quality suggest that it is possible to prepare rice pasta
297 directly from the extrusion of parboiled rice kernels previously hydrated and
298 maintained moistened for at least 3 hours before processing, as suggested by the water
299 status of soaked kernels during the resting phase. The cooking behavior was not
300 negatively affected by the processing, suggesting that this new process might be
301 applied to other raw materials, and represents a simplification of the pasta-making
302 process from raw materials different from wheat flour and/or semolina. The
303 consequent economical benefits could be of great interest especially in developing
304 Countries. Further studies will focus on the optimization of parboiling processing with
305 the aim of decreasing the time required for kernels hydration (3 h), to make the
306 process more suitable for industrial scale-up.

307 **Acknowledgments**

308 Authors wish to acknowledge Dr. Flavio Mazzini and Mr Grugni (former Riso Viazzo
309 s.r.l., Crova, Italy) for providing the rice kernels and Dr. Rosita Caramanico (CREA,
310 Research Center for Engineering and Agro-Food Processing, Milan, Italy) for
311 technical assistance.

312 **Conflict of interest**

313 There is no conflict of interest.

314 **References**

315 Barbiroli, A., Bonomi, F., Casiraghi, M. C., Iametti, S., Pagani, M. A., &
316 Marti, A. (2013). Process conditions affect starch structure and its interactions with
317 proteins in rice pasta. *Carbohydrate Polymers*, *92*, 1865-1872.

318 Bhattacharya, K. R., & Ali, S. Z. (1985). Changes in rice during parboiling
319 and properties of parboiled rice. In Y. Pomeranz (Eds.), *Advances in cereal science
320 and technology* (pp. 105-167). St. Paul: The American Association of Cereal Chemist,
321 Inc.

322 Bhattacharya, M., Zee, S. Y., & Corke, H. (1999). Physicochemical properties
323 related to quality of rice noodles. *Cereal Chemistry*, *76*, 861–867.

324 Bhattacharya, K. R. (2004). Parboiling of rice. In E. T., Champagne (Eds.),
325 *Rice: chemistry and technology* (pp. 329-404). St. Paul: The American Association of
326 Cereal Chemists, Inc.

327 Bonomi, F., D'Egidio, M.G., Iametti, S., Marengo, M., Marti, A., Pagani,
328 M.A., & Ragg, E. (2012). Structure-quality relationship in commercial pasta: a
329 molecular glimpse. *Food Chemistry*, *135*, 348-355.

330 Cabrera-Chavez, F., Calderon de la Barca, A.M., Islas-Rubio, A.R., Marti, A.,
331 Marengo, M., Pagani, M.A., Bonomi, F., & Iametti, S. (2012). Molecular
332 rearrangements in extrusion processes for the production of amaranth-enriched,
333 gluten-free rice pasta. *LWT-Journal of Food Science and Technology*, *47*, 421-426.

334 Carini, E., Curti, E., Littardi, P., Luzzini, M., & Vittadini, E. (2013). Water
335 dynamics of ready to eat shelf stable pasta meals during storage. *Innovative Food
336 Science and Emerging Technologies*, *17*, 163–168

337 Casiraghi, M. C., Brighenti, F., Pellegrini, N., Leopardi, E., & Testolin, G.
338 (1993). Effects of processing on rice starch digestibility evaluated by in vivo and in

339 vitro methods. *Journal of Cereal Science*, 17, 147-156.

340 Gruwel, M. L., Chatson, B., Yin, X. S., & Abrams, S. (2001). A magnetic
341 resonance study of water uptake in whole barley kernels. *International Journal of*
342 *Food Science & Technology*, 36, 161-168.

343 Hong, Y. S., Hong, K. S., Lee, E. S., Cho, J. H., Lee, C., Cheong, C., & Lee,
344 C. H. (2009). MR imaging and diffusion studies of soaked rice. *Food Research*
345 *International*, 42, 237-245.

346 Horigane, A. K., Kawabuchi, M., Uchijima, S., & Yoshida, M. (2009). Effects
347 of seasonings on physical properties and MRI T2 map of cooked spaghetti. *Food*
348 *Research International*, 42, 41–50.

349 Lai, H. M. (2002). Effects of rice properties and emulsifiers on the quality of
350 rice pasta. *Journal of the Science of Food and Agriculture*, 82, 203-216.

351 Lamberts, L., Brijs, K., Mohamed, R., Verhelst, N., & Delcour, J. A. (2006).
352 Impact of browning reactions and bran pigments on color of parboiled rice. *Journal of*
353 *Agricultural and Food Chemistry*, 54, 9924-9929.

354 Lucisano, M., Cappa, C., Fongaro, L., & Mariotti, M. (2012). Characterisation
355 of gluten-free pasta through conventional and innovative methods: evaluation of the
356 cooking behaviour. *Journal of Cereal Science*, 56, 667-675.

357 Mariotti, M., Iametti, S., Cappa, C., Rasmussen, P., & Lucisano, M. (2011).
358 Characterisation of gluten-free pasta through conventional and innovative methods:
359 evaluation of the uncooked products. *Journal of Cereal Science*, 53, 319-327.

360 Marti, A., Abbasi Parizad, P., Marengo, M., Erba, D., Pagani, M. A., &
361 Casiraghi, M. C. (2017). In vitro starch digestibility of commercial gluten-free pasta:
362 the role of ingredients and origin. *Journal of Food Science*, 82, 1012-1019.

363 Marti, A., Barbiroli, A., Marengo, M., Fongaro, L., Iametti, S., & Pagani,

364 M.A. (2014). Structuring and texturing gluten-free pasta: egg albumen or whey
365 proteins? *European Food Research Technology*, 238, 217-224.

366 Marti, A., Caramanico, R., Bottega, G., & Pagani, M.A. (2013). Cooking
367 behaviour of rice pasta: effect of thermal treatments and extrusion conditions. *LWT –*
368 *Food Science and Technology*, 54, 229-235.

369 Marti, A., Fongaro, L., Rossi, M., Lucisano, M., & Pagani, M.A. (2011c).
370 Quality characteristics of pasta enriched with buckwheat flour. *International Journal*
371 *of Food Science and Technology*, 46, 2393-2400.

372 Marti, A., Pagani, M.A., & Seetharamna, K. (2011a). Understanding starch
373 organisation in gluten-free pasta from rice flour. *Carbohydrate Polymers*, 84, 1069–
374 1084.

375 Marti, A., Pagani, M.A., & Seetharamna, K. (2011b). Characterizing starch
376 structure in a gluten-free pasta by using iodine vapor as a tool. *Starch/Starke*, 63,
377 241–244.

378 Marti, A., Seetharaman, K., & Pagani, M.A. (2010). Rice-based pasta: a
379 comparison between conventional pasta-making and extrusion-cooking. *Journal of*
380 *Cereal Science*, 52, 404-409.

381 Posner, E. S., & Hibbs, A. N. (2005). Wheat flour milling (Second Edition).
382 St. Paul: The American Association of Cereal Chemists, Inc.

383 Takeuchi, S., Maeda, M., Gomi, Y., Fukuoka, M., & Watanabe, H. (1997).
384 The change of moisture distribution in a rice grain during boiling as observed by
385 NMR imaging. *Journal of Food Engineering*, 33, 281-297.

386 **Captions**

387 **Fig. 1.** MRI images (proton density) of parboiled rice at increasing time after initial
388 soaking in water at 50°C. Labels 1 and 2 (in the image at time = 20 min) indicate rice
389 kernels considered for further numerical analysis.

390

391 **Fig. 2.** Parametric MRI images (T_2) of parboiled rice measured at increasing times
392 after initial soaking in water. T_2 values are color-coded from blue ($T_2= 5\text{ms}$) to red
393 ($T_2=53\text{ms}$). Hydration times (min) are shown on top. The rice kernel is the same as
394 that one labelled “1” in Fig. 1

395

396 **Fig. 3.** A: Time course of MRI signal along the two principal directions, 1 (long axis)
397 and 2 (short axis), in selected slices of individual rice kernels (labelled 1 and 2 in
398 Fig. 1. B: Time course of the area containing tightly bound water ($T_2<15\text{ms}$) in a
399 selected rice kernel. Data were collected from the slice depicted in Fig. 2. Continuous
400 lines are drawn from a non-linear least squares fitting analysis.

401

402 **Fig. 4.** MRI images on selected slices (0.3 mm thickness) of PaRF (left) and PaK
403 (right) pasta samples after 15 min cooking. Top: proton density image, color-coded
404 from blue (low signal) to red (high signal); bottom: T_2 distribution (parametric
405 image). T_2 values are color-coded from blue ($T_2= 5\text{ms}$) to red ($T_2=53\text{ms}$).

406

407 **Fig. 5.** T_2 distribution (pixel count) of the MRI T_2 parametric images shown in Fig.6
408 for PaRF (left) and PaK (right) cooked pasta samples. Letters a, b and c denote the
409 three main regions with different water mobility.

410

411 **Supplementary material**

412 **Fig. S1.** Processing conditions for experimental rice pasta-making from rice kernels
413 and rice flour.

414

415 **Fig. S2.** Pasting properties of PaRF (full line) and PaRK (black dashed line).

416 Temperature profile in grey full line.

417 PaRF, gluten-free pasta prepared from parboiled rice flour

418 PaRK, gluten-free pasta prepared directly from from parboiled rice kernels

419

420

421

422

Table 1. Pasta color, cooking behavior, and pasting properties

		PaRF	PaRK
Color	Luminosity (L^*)	80.9 ± 0.44	81.0 ± 0.32
	Redness (a^*)	0.30 ± 0.09 ⁺	0.48 ± 0.11
	Yellowness (b^*)	15.1 ± 0.70 ⁺	13.6 ± 0.26
Optimal Cooking Time (min)		15	15
Water Absorption (g/100g)		95.4 ± 5.4	91.9 ± 4.2
Cooking losses (g/100g)		12.0 ± 3.6	11.1 ± 2.8
Texture	Firmness (N)	1337.8 ± 144.6	1431.7 ± 134.9
	Compression Energy (N*mm)	5256.0 ± 521.4	5403.7 ± 599.8
	Shear Force (N)	896.4 ± 31.0 ⁺	1066.5 ± 36.5
Pasting properties	Pasting Temperature (°C)	62.4 ± 0.30 ⁺	55.6 ± 0.01
	Maximum Viscosity (BU)	176.5 ± 5.5 ⁺	258.5 ± 6.5
	Partial Setback (BU)	184.5 ± 0.71 ⁺	286.0 ± 11.3
	Final Setback (BU)	246.0 ± 8.5 ⁺	364.0 ± 4.2

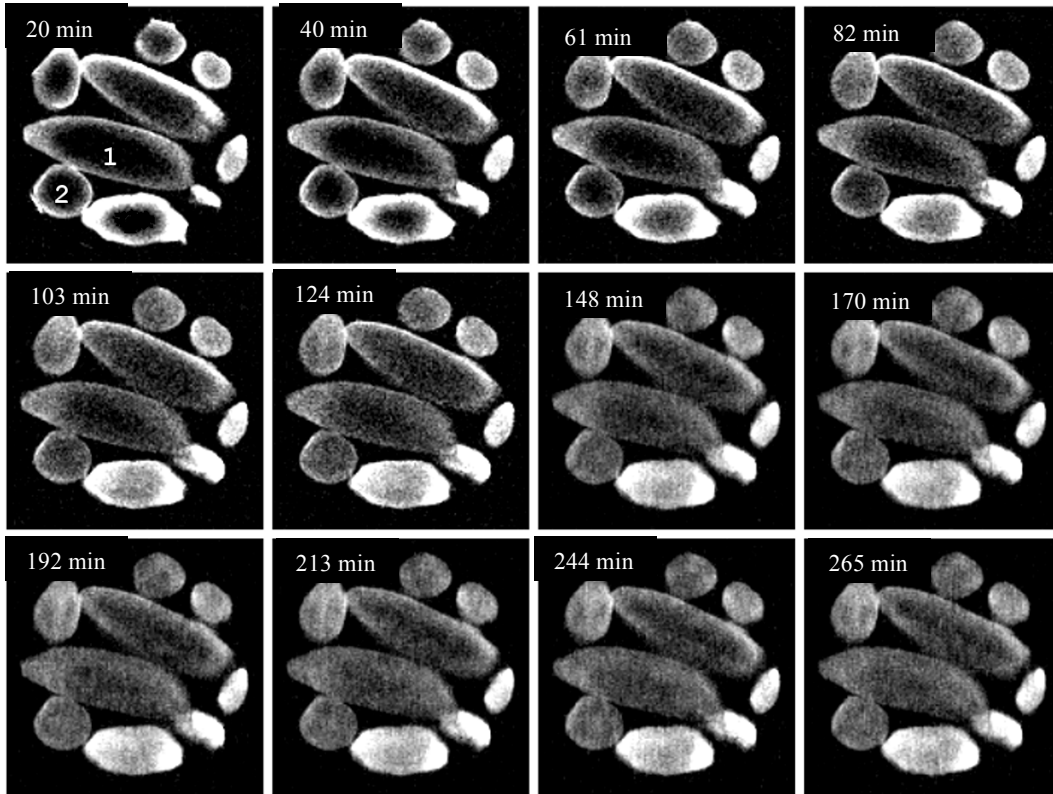
423

424 ⁺ significantly differences (t-test, p<0.001)

425 Pasting temperature, temperature at which an initial increase in viscosity occurs.

426 Maximum viscosity, viscosity achieved at 95 °C.

427 Partial Setback, difference between the viscosity at 50 °C and the viscosity reached
428 after the holding period at 95 °C).429 Final Setback viscosity, difference between the final viscosity at 30 °C and the
430 viscosity reached at 50 °C).431 PaRF, gluten-free pasta prepared from rice flour; PaRK, gluten-free pasta prepared
432 directly from from rice kernels

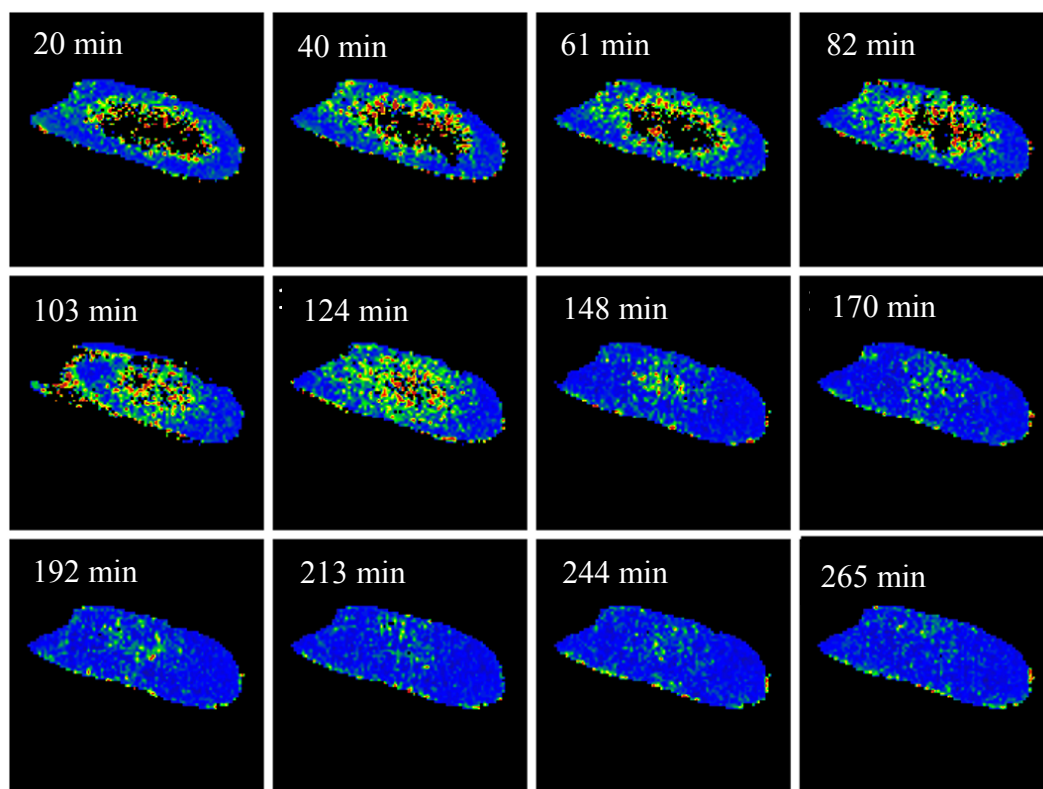


433

434 Fig. 1.

435

436

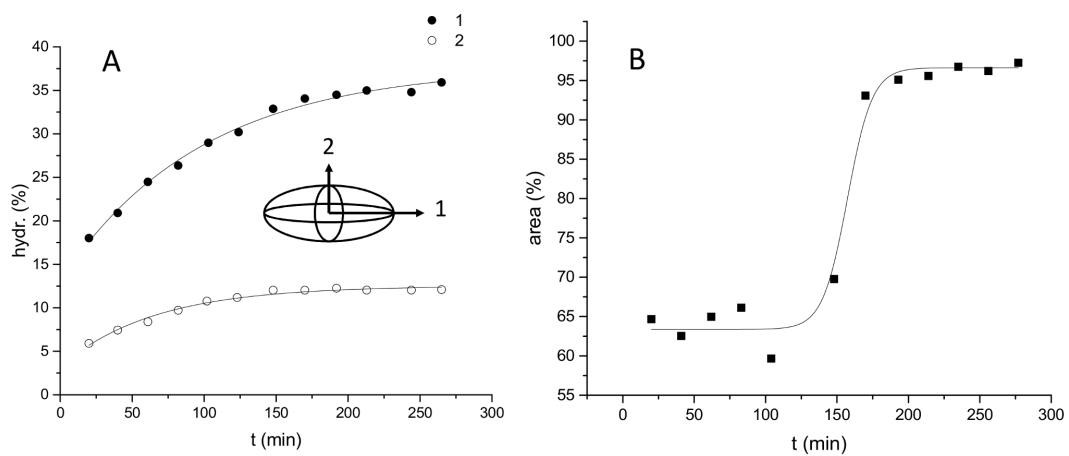


437

438 Fig. 2.

439

440



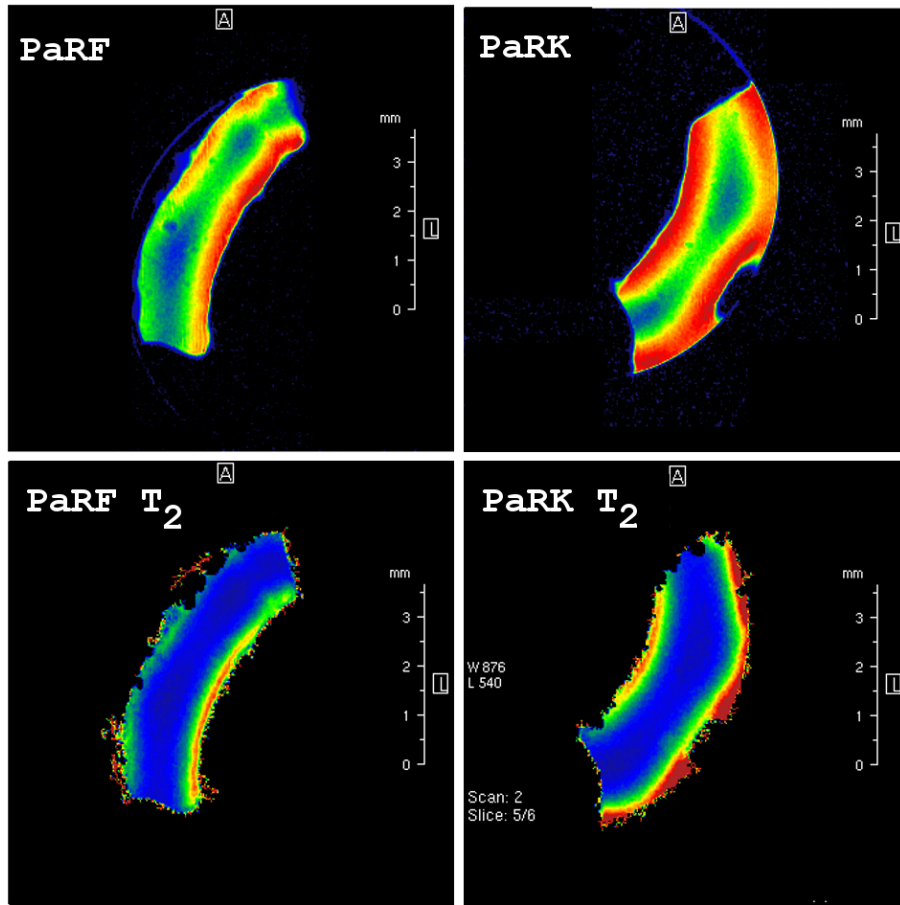
441

442 Fig. 3.

443

444

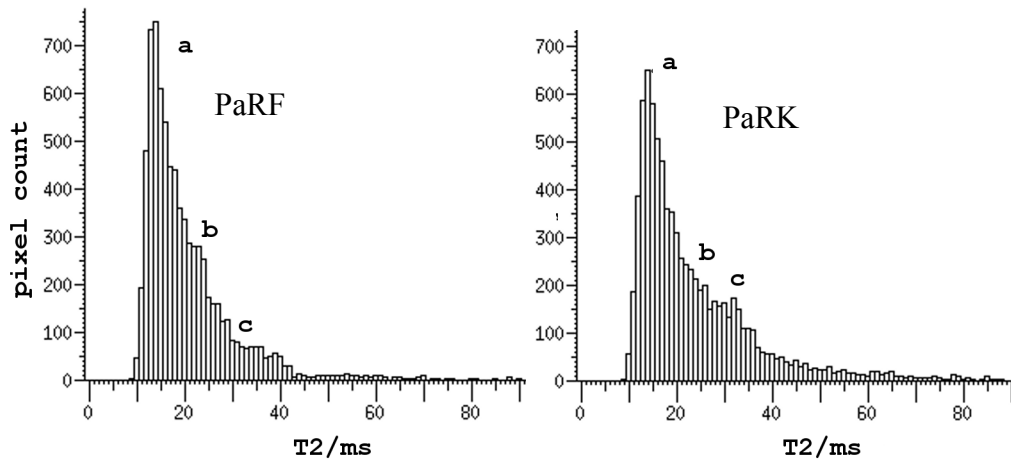
445



446

447 Fig. 4.

448



449

450 Fig. 5.

451